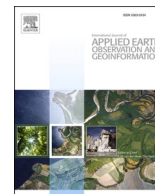


Contents lists available at [ScienceDirect](https://www.sciencedirect.com)

# International Journal of Applied Earth Observations and Geoinformation

journal homepage: [www.elsevier.com/locate/jag](http://www.elsevier.com/locate/jag)

## Prediction of insect-herbivory-damage and insect-type attack in maize plants using hyperspectral data

Danielle Elis Garcia Furuya<sup>a</sup>, Lingfei Ma<sup>b,\*</sup>, Mayara Maezano Faita Pinheiro<sup>a</sup>, Felipe David Georges Gomes<sup>a</sup>, Wesley Nunes Gonçalves<sup>c</sup>, José Marcato Junior<sup>c</sup>, Diego de Castro Rodrigues<sup>d</sup>, Maria Carolina Blassioli-Moraes<sup>e</sup>, Mirian Fernandes Furtado Michereff<sup>e</sup>, Miguel Borges<sup>e</sup>, Raúl Alberto Alaumann<sup>e</sup>, Ednaldo José Ferreira<sup>f</sup>, Lucas Prado Osco<sup>g</sup>, Ana Paula Marques Ramos<sup>a,h</sup>, Jonathan Li<sup>i</sup>, Lúcio André de Castro Jorge<sup>f</sup>

<sup>a</sup> Program of Environment and Regional Development, University of Western São Paulo, Presidente Prudente, Brazil

<sup>b</sup> Engineering Research Center of State Financial Security, Ministry of Education, Central University of Finance and Economics, Beijing 102206, China

<sup>c</sup> Faculty of Engineering, Architecture, and Urbanism and Geography, Federal University of Mato Grosso do Sul, Campo Grande, Brazil

<sup>d</sup> Department of Computing, Federal Institute of Education of Tocantins, Dianópolis, Brazil

<sup>e</sup> National Research Center of Development of Genetic Research and Biotechnology, Brazilian Agricultural Research Agency, Brasília, Brazil

<sup>f</sup> National Research Center of Development of Agricultural Instrumentation, Brazilian Agricultural Research Agency, São Carlos, Brazil

<sup>g</sup> Faculty of Engineering and Architecture and Urbanism, University of Western São Paulo, Presidente Prudente, Brazil

<sup>h</sup> Program of Agronomy, University of Western São Paulo, Presidente Prudente, Brazil

<sup>i</sup> Department of Geography and Environmental Management, University of Waterloo, Waterloo, Canada

### ARTICLE INFO

#### Keywords:

Proximal hyperspectral sensing  
Precision agriculture  
Random forest

### ABSTRACT

Accurately detecting the insect damage caused in plants might reduce losses in crop yields. Hyperspectral data is a well-accepted data source to attend this issue. However, due to their high dimensional, both robust and intelligent methods are required to extract information from these datasets. Therefore, we explore the processing of hyperspectral data with artificial intelligence methods joined with clustering techniques to detect insect herbivory damage in maize plants. We measured the leaf spectral response from three different groups of maize plants: control (undamaged plants); damaged by Spodoptera frugiperda herbivory, and damaged by Dichelops meiacanthus. Data were collected with a FieldSpec 3.0 Spectroradiometer from 350 to 2500 nm for eight consecutive days. We adjusted eight machine learning methods. We also determined the most contributive wavelengths to differentiate undamaged from damaged plants by insect herbivore attack using clustering strategy. For that, we applied the clusterization method based on a self-organizing map (SOM). The Random Forest (RF) model is the overall best learner, and up to the 5th day of analysis represents the most adequate day to segregate maize undamaged from damaged maize. RF was able to separate the three groups of treatments with an F1-measure of up to 96.7% (Recall of 96.7% and Precision of 96.7%). Additionally, we found out that the most representative spectral regions are located in the near-infrared range. Our approach consists of an original contribution to early differentiate the undamaged plant from the damaged one due to insect-attack, highlighting the most contributive wavelengths to map this occurrence.

### 1. Introduction

One of the major factors that impact a country's economic development is its agronomic sector since it is responsible for, among others, raw material, employment generation, and both human and animal food

production. Several issues can impact a crop yield rate, chemical fertilizer overutilization, presence of chemicals in water supply, uneven distribution of rainfall, soil fertility differences, and the attack of pests or diseases in plants (Singh et al., 2020). Plant diseases are described as some of modification that hampers the normal processes in their healthy

\* Corresponding author.

E-mail address: [l53ma@cufe.edu.cn](mailto:l53ma@cufe.edu.cn) (L. Ma).

<https://doi.org/10.1016/j.jag.2021.102608>

Received 4 August 2021; Received in revised form 27 October 2021; Accepted 27 October 2021

0303-2434/© 2021 Published by Elsevier B.V. This is an open access article under the CC BY-NC-ND license (<http://creativecommons.org/licenses/by-nc-nd/4.0/>).

development (Singh et al., 2020). Not only the disease but also insect-damage occurrences significantly endangers agriculture around the world (Zhang et al., 2019) being usually associated with huge economic losses. To illustrate this scenario, for 12 major maize-growing countries, insect-damage costs a total of 1–4 billion dollars in lost crops per year (Silver, 2019).

Maize is a versatile plant, used both to feed human and domestic animals, making maize one of the most important sources of income in family farms. Brazil is the third-largest producer of maize in the world. The last crop season (2019/2020) represents a record production with 105 million tons approximately, resulting in an increase of 2.6% in relation to the previous one (CONAB, 2020). In China, the second-largest producer of maize in the world, caterpillars that ravage crops are advancing across fields and threatening this nation's vast supply of maize (Silver, 2019). Africa, where the pest arrived in 2016, and southern Asia have also reported a recent outbreak of bugs, causing maize yield losses surpassing 50% (Silver, 2019). Since maize cultivation is still a monoculture type of practice in many areas around the world, as well as occupying large portions lands, it is often susceptible to infestations and diseases. There are more than 40 species of insects recorded on maize crop, among them are the maize stalk borer (*Busseola fusca*), spotted stalk borer (*Chilo partellus*), various termite species (*Macrotermes* and *Microtermes* spp.), and a more recent invasive species, the Spodoptera frugiperda (J. E. Smith) (Lepidoptera: Noctuidae), commonly named fall armyworm (FAW) (Assefa and Ayalew, 2019). A strategy to minimize both qualitative and quantitative losses in crop yield refers to early and accurate detection of insect-damage caused in plants (Mahlein, 2016). However, several examples about the traditional approaches for monitoring plants in the field is labor-intensive, being prone to be subjective, and generally shows low efficiency (Zhang et al., 2019; Mahlein, 2016).

One of the main reasons behind insect infestation in farmlands across the planet involves disregard for control measures, the presence of varieties which are susceptible to pest attack, lack of crop rotation practices; imbalanced fertilization, as well as the inappropriate use of pesticides and others (Oliveira et al., 2014; Zhang et al., 2019; Tageldin et al., 2020). This procedures can result in impacts upon the farmland, one of which the uncontrolled presence of pests and insects. As traditional approaches, mechanical, chemical and biological controls' practices employ a series of techniques that aim to maintain the pest density at a lower level than that which would occur in the absence of its natural enemies around the area. However, such methods although are capable of controlling said pests, are often misused and can lead to different outcomes (Oliveira et al., 2014; Zhang et al., 2019; El-Ghany et al., 2020). Some of them are effective at different scales, and some are labor-intensive, onerous and costly for most producers. Because of that, novel methods that employ a more indirect approach, as well as less aggressive, for detecting the damage, are being prone to use in recent researches in the precision agriculture field.

Remote sensing is a promising strategy for managing crops because they can provide directly non-contact and spatially continuous monitoring of diseases and pests efficiently (Osco et al., 2019; Zhang et al., 2019). The principle of remote sensing is that all targets (e.g. soil, vegetation, water, etc.) on the terrestrial surface reflect and emit electromagnetic energy in specific wavelengths owing to difference in their chemical, inner physical, and surface properties (roughness) (Jensen, 2014). In a hyperspectral context, this means measuring hundreds of narrow bands within the electromagnetic spectrum. In this regard, the spectroscopy area refers to the method of obtaining the hyperspectral characteristics of a target regarding radiation flux intensity emitted or reflected by its constituents at different wavelengths to provide a precise fingerprint of a target (e.g. a plant) (Jensen, 2014). For the last decades, many studies have proved the potential of remote sensing in the precision agriculture area, mainly for plant disease detection (Asner, 1998; Liu et al., 2018; Zhang et al., 2019; El-Ghany et al., 2020; Zhang et al., 2020). A study (Asner, 1998) demonstrated that various biophysical and

biochemical factors affect plant canopy reflectance, and show that an adequate sampling (spectral, angular, and temporal) of the optical (400–2500 nm) spectrum is required. Methods for modeling insect-damage caused by plants can be divided into traditional statistical analysis to even innovative artificial intelligence approaches like machine learning and deep learning (Zhang et al., 2019). Artificial intelligence techniques may be an interesting approach mainly because of its robustness to evaluate high dimensional data, such as data collected from proximal sensing equipment.

Studies investigated remote sensing and artificial intelligence techniques in the agriculture area (Berger et al., 2020; Osco et al., 2020a; Ramos et al., 2020). As examples, (Singh et al., 2009) investigated the potential of near-infrared hyperspectral (1000 to 1600 nm) images processed by linear discriminant analysis and quadratic discriminant analysis for the detection of insect-damaged wheat kernels and pointed out that methods correctly classified 85–100% healthy and insect-damaged wheat kernels. (Wang et al., 2011) adopted hyperspectral (400 to 720 nm) images processed with the stepwise discriminant analysis for the detection of external insect damage in jujube fruits, and the overall classification accuracy was about 97.0%. (Liu et al., 2018) measured the hyperspectral reflectance (350 to 2,500 nm) of symptomatic and asymptomatic rice leaves infected by four different diseases. Based on probabilistic neural network classifiers, it was concluded, with the mean overall accuracy upper to 91%, that symptomatic and asymptomatic rice leaves can be discriminated using hyperspectral reflectance measurements only.

An investigation (Kandpal et al., 2015), applying the partial least squares discriminant analysis in hyperspectral (1100 to 1700 nm) images of the short-wave infrared region, was able to demonstrate, with an accuracy upper to 96%, aflatoxin contamination on corn kernels. (Abdulridha et al., 2019) applied two machine learning algorithms, radial basis function (RBF) and K-nearest neighbor (KNN), in hyperspectral (400 to 1,000 nm) images for the detection of citrus canker in several disease development stages (i.e., asymptomatic, early, and late symptoms) on Sugar Belle leaves and immature (green) fruit, and the overall classification accuracy of both methods was higher than 94%. (Nyabako et al., 2020) developed decision-tree algorithms to predict the level of *P. truncatus* infestation and associated damage of maize grain in smallholder farmer stores. *P. truncatus* population size prediction, the model performance was weak ( $r = 0.43$ ) because of the complicated sampling and detection of the pest and eight-week long period between sampling events. To grain damage prediction, the model had a stronger correlation coefficient ( $r = 0.93$ ) being considered a good estimator of damages in grain caused by insects. (Tageldin et al., 2020) investigated several learning algorithms to predict the cotton leafworm (*Spodoptera littoralis*) plant infestation in the greenhouses and found that the XGBoost algorithm was the most effective algorithm achieving a prediction accuracy of 84%.

As mentioned, hyperspectral datasets provide high-dimensional data merged into a data vector, and occasionally require the application of techniques for datasets reduction or clustering. A clustering method like the Self-Organizing Map (SOM) is a promissory alternative. SOM can dimensionally organize complex data into clusters according to their relationships, being a highly appropriate method to solve difficult high-dimensional and nonlinear problems, such as feature extraction and image classification (Li et al., 2019). A main feature of the SOM is to compose a nonlinear mapping of a high-dimensional input space to a typically 2-D grid of artificial neural units (Kohonen, 1982; Kohonen, 2001). For that, SOM is based on an artificial neural network trained based on unsupervised learning, consisting of a two-layer, an input layer and an output layer known as the Kohonen layer (Kohonen, 1982; Kohonen, 2001). The literature review presents many studies using the SOM architecture in different applications, including remote sensing and agriculture-related problems (Li et al., 2019; Rivas-Tabares et al., 2020). Although the main concept behind it may be appropriate to different intakes in the hyperspectral data domain, here we discuss its

implications in plant monitoring, more specifically maize, due to its necessity in providing methods to infer insect damage. This is important since precision agriculture practices involves identifying the most expressed wavelengths to a given problem. Maize are susceptible to some plagues, and its monitoring is a necessity in most farmlands, specially for tropical and sub-tropical zones.

The SOM method is in widespread use across several disciplines. However, its potential for clustering the more adequate spectral regions to detect insect attacks in crops like maize, based on hyperspectral datasets analysis is still unexplored. Adopting robust methods to deal with the high-dimensional characteristics of HSI data when the ranking and SOM approach are combined refers to an original and important contribution that might be assist agricultural management in a rapid and in situ manner. The ranking approach has been adopted, for example, to identify the individual contribution of each spectral information, collected by remote sensing, included in a learning model to solve precision agriculture problems (Osco et al., 2020a; Ramos et al., 2020). The ranking method calculates the increased or decreased difference in the performance of the algorithm against the performance of a baseline method concerning a given variable, and this returns a metric score for the individual input variables, thus indicating the contribution of each index into the model. Therefore, we propose an approach based on artificial intelligence techniques (machine learning and deep learning) to predict whether the plant is attacked or not by insects using HSI dataset. The results obtained showed that the reflectance measures differentiate the herbivore-type of damage, i.e, differentiate the herbivory provoked by larvae of *Spodoptera frugiperda*, a chewing insect, from the herbivory provoked by the stink bug *Dichelops melacanthus*, a sucking feeding insect. In short, here we present:

1. The performance of different machine learning approaches;

2. The impact of a day-by-day analysis into the prediction, and;
3. A framework to identify important spectral regions for this prediction using the ranking and SOM approach.

## 2. Materials and method

The method (Fig. 1) was divided into the following main phases: 1) proximal sensing data acquisition; collected from different maize plants during different days in-field conditions; 2) data process and organization; separated into multiple datasets to be evaluated by the models; 3) machine and deep learning evaluation; used to indicate the more appropriate to predict the insect-damage in this type of data; 4) temporal analysis comparison; implemented to determine the impact on an individual analysis of the overall best, predefined in the previous step; 5) ranking and clustering with SOM of the contribution of wavelengths to the models' performance; proposed to the appropriate spectral regions to separate insect-damage from undamaged plants and to differentiate the insect-type damage in maize plants.

### 2.1. Insects and plants

*Spodoptera frugiperda* were maintained in separate environmental rooms at  $27 \pm 1$  °C, with  $65 \pm 10\%$  relative humidity and a 14 h photoperiod. *S. frugiperda* larvae were obtained from a laboratory colony maintained at Embrapa Genetic Resources and Biotechnology in Brasília, DF, Brazil. The larvae were reared in plastic containers on an artificial diet based on beans (*Phaseolus vulgaris*). Second instar larvae (Schmidt et al., 2009) were used in experiments and starved for 24 h before the experiment. *Dichelops melacanthus* individuals were obtained from a laboratory colony started from adults collected in soybean fields near Embrapa Genetic Resources and Biotechnology, Brasília,

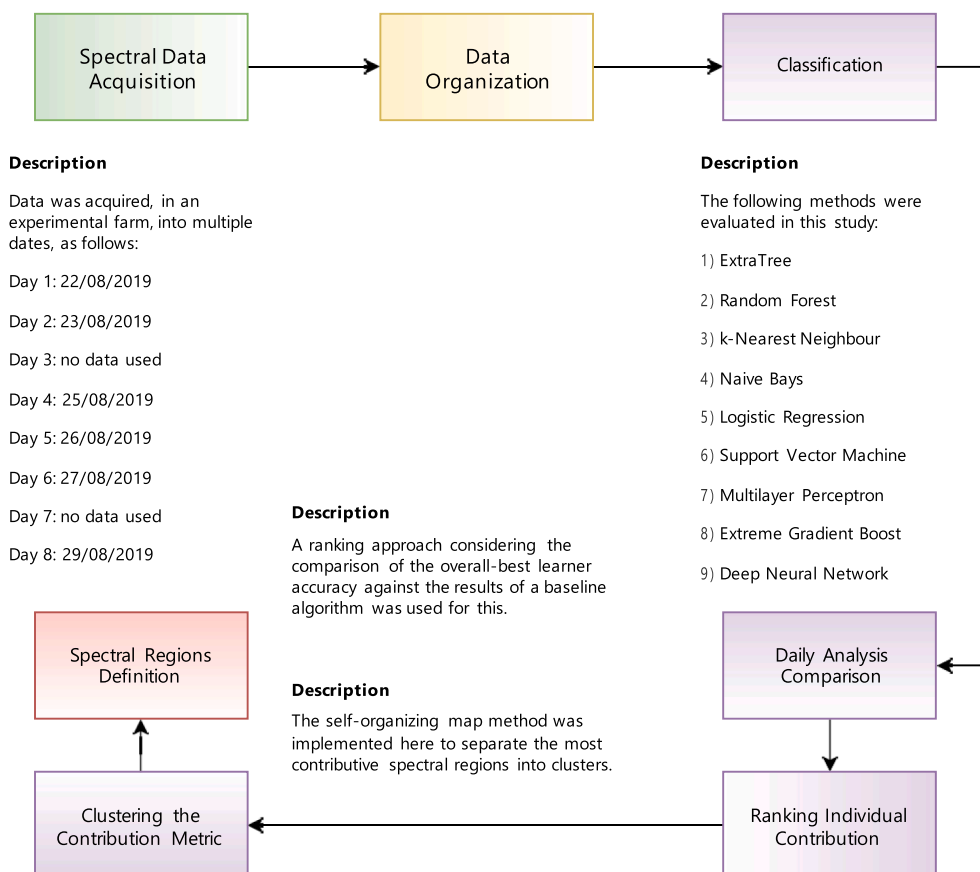


Fig. 1. The summarized steps of the framework developed in this study.

Brazil (15°47'0''J<sup>S</sup>, 47°55'0''J<sup>W</sup>).

Stink bugs were reared in 8 L plastic containers on a diet of soybean seeds (cv Conquista), sunflower seeds (*Helianthus annuus*), raw peanuts (*Arachis hypogaea*), fresh green beans (*Phaseolus vulgaris*), and water. The food supply was renewed twice a week. To provide an oviposition substrate and shelter for the bugs, a 15 cm<sup>2</sup> piece of nylon mesh screen was placed inside the cage. They were kept in a controlled environment room at L14: D10 photoperiod, 26 ± 0.3 °C and 70 ± 10% r.h.

Maize seeds were obtained from Germplasm Bank of Embrapa Maize and Sorghum in Sete Lagoas, MG, Brazil (19°27'57''J<sup>S</sup> and 44°14'48''J<sup>W</sup>) and germinated on damp paper. After 4 days, the seeds were transplanted to pots with a mixture of soil and organic substrate (in a proportion of 1:1 w/w) and kept in a greenhouse (14 h photoperiod). The plants used in the experiments were grown for 9–10 days after emergence and had three fully expanded leaves.

## 2.2. Experimental area and data acquisition

The semifield experiments were conducted in an external area of our laboratory in Brasilia with natural light. The plants of maize received one of the following treatments: 1) undamaged plants (UDP) (did not receive the treatment), 2) two (2) 2nd instar larvae of *S. frugiperda* herbivory damaged plants (Sf-HDP) (N = X for each treatment) and 3) two (2) adult females of *Dichelops melacanthus* herbivory damaged plants (Dm-HDP). Reflectance data from plants under these three treatments were collected from 09 to 15 h. The data was acquired over 8 days, except for day 3 and 7, which were collected outside the 09 to 15 h interval, thus, not used in this study. The combined measurements from all eight days resulted in 1,429 samples (instances) for the models.

The spectral reflectance from the plants was collected with a compact, field-portable, and precision instrument with a spectral range of 350–2,500 nm, FieldSpec 3.0 ASD spectroradiometer, at daylight conditions, in a rapid data collection time of 0.1 s per spectrum. The sampling interval is 1.4 nm for the spectral region 350–1,000 nm and 2 nm for the spectral region 1,000–2,500 nm. We used a small size of the pistol grip and 8 grades for optics around 50 cm far from the samples and material with approximately 100% reflectance across the entire spectrum as a white reference panel or white reference standard.

We connected the apparatus to a portable microcomputer, where data was stored. The reflectance spectrum ( $\rho$ ) was calculated with the division of the radiance from the target (LT) (in this case, the plant) by the amount of radiance reflected from a reference sample (Lr). This was multiplied by a correction factor (K), which corresponds with the ratio between the solar irradiance to a reference plate exitance (Jensen, 2014). This process can be summarized by the Eq. (1) below:

$$\rho_T = \frac{L_T}{L_r} \times K \quad (1)$$

At each time of acquisition the reflectance was calibrated with the white standard. Since the wavelengths are interpolated at 1 nm, the final product of the spectral reading is a high-dimensionality dataset with 2,150 bands. We then identified low signal-to-noise spectral regions, both from the beginning of the equipment, at the 350 and 390 nm, and others mostly related to atmospheric conditions and equipment interference, from 1,350 to 1,410 nm, 1,820 to 1,940 nm, and 2,460 to 2,500 nm. This resulted in 1,694 bands to be incorporated into the analysis as input variables. The processed data, in reflectance value, was organized into separated subsets.

Before the analysis, we reordered the spectral wavelengths into columns, to be used separately by the models. The training and testing samples were separated according to the measured plant. We previously labeled every measure plant and, since multiple leaves from the same plant were measured, the training and testing samples were divided according to a label previously given to each leaf, indicating its respective plant. This was necessary because a random division could potentially result in the spectral reading of different leaves from the

same plant being in both training and testing subsets. In this sense, from the 1,429 samples collected, a total of 1,001 leaves were used for training, while the remaining 408 leaves were used for the testing set.

## 2.3. Insect herbivory damage classification

To determine the overall learner to model the spectral configuration-sets, we choose 8 algorithms based upon their theoretical characteristics and state-of-the-art usage. The algorithms were: ExtraTree (ExT); k-Nearest Neighbour (kNN); Logistic Regression (LoR); Multi-Layer Perceptron (MLP); Naive Bayes (NB); Random Forest (RF); Support Vector Machine (SVM) and; Extreme Gradient Boost (XGB). We also used a deep neural network (DNN) method to evaluate the ability of a deep learning model to classify this data. In an experimental initial phase, we evaluated the individual performance of the algorithms to determine whether a fine-tuning of its parameters was necessary. Upon comparisons of fine-tuning methods with the algorithm's baseline, we verified that no improvement was obtained in relation to the processing time needed to perform the classifications.

While DNNs are, traditionally, similar to ANNs, they are considered more robust than a common ANN specially because of its complexity, being defined as a learning method with multiple levels of representation (Lecun, 2015; Osco et al., 2021). In our experiment, the default values of the implemented libraries were adopted. The MLP was constructed with one hidden layer, in a feed-forward manner, with a learning rate of 0.05, momentum of 0.1, using the Adam solver and a sigmoid function as its activation function. As for the DNN, we used the Adam optimizer and adopted an adaptive learning rate with a sparse categorical cross-entropy loss function. For the hidden-layers, we used two layers with 128 neurons and two layers with 32 neurons, adopting a dropout of 20% on each one. All hidden layers were assigned a ReLU activation function. A dense final layer was added with the softmax function with 3 units. A total of 800 epochs were evaluated and the deviance criteria were used to determine the necessary amount of epochs.

The machine learning models were applied through the open-source software Weka 3.9.4, using integrated libraries from the R, XGBoost and Scikit-Learn packages. The deep learning model was created with the Tensorflow package, in Python 3.9. The computational analysis was conducted in two different phases: In the first phase, we determine the overall best learner to model the spectral data, and investigated the impact of different daily measurements on this; in the second phase, we modeled the damage according to its origin type (*S. frugiperda* or *D. melacanthus*). The datasets are summarized in Table 1. The ‘‘Herbivory

**Table 1**

Configuration-sets used to predict insect damage and separate insect damage types. MAC = Multiple Algorithm Comparison; SAC = Single Algorithm Analysis; and RSOM = Ranking and Self-Organizing Map.

Dataset	UDP (n)	Herbivory damaged (n)	Total (n)	Sf-HDP (n)	Dm-HDP (n)	Experiment
Total	464	855	1319	505	350	MAC
Analysis						
Day 1	104	180	284	100	80	SAC
Day 2	150	265	415	185	80	SAC
Day 4	50	120	170	70	50	SAC
Day 5	60	90	150	50	40	SAC
Day 6	50	100	150	50	50	SAC
Day 8	50	100	150	50	50	SAC
UDP vs Sf-HDP	60	50	110	50	0	RSOM
UDP vs Dm-HDP	60	40	100	0	40	RSOM
Sf-HDP vs Dm-HDP	0	90	90	50	40	RSOM

Damaged” group corresponds to the sum of observations of larvae (Spodoptera frugiperd) and stink-bugs (Dichelops melacanthus) groups. The Total Analysis group is the sum from Day 1 to 8 groups.

The comparison with multiple machine learning algorithms was performed using all reflectance measurements acquired during 8 days of analysis. For this, the 8 algorithms were compared after 100 validation results. The same data subsets were considered for every classification. The classification metrics evaluated in this study were Precision, Recall, and F-measure. We also used the True-Positive and False-Positive Rates and the Receiver Operating Characteristic (ROC) curve for each classifier. After defining the overall best learner, a daily comparison with data collected from the beginning to the end of the experiment (days 1 through 8) was used as separated inputs for the classification task. The strategy described in the previous step, for processing and evaluating the performance of the algorithm, was also adopted. This helped define the impact of the continuous attack of the insets into the analysis of the spectral behavior of the maize plants. With that, it was possible to indicate the most discrepant days of analysis since the beginning of the infestation.

### 2.4. Ranking and clustering of spectral data

To calculate the potential of every wavelength used as input for the overall best classifier, we adopted a ranking approach. This ranking approach consists of a direct comparison between the used classifiers’ accuracy, obtained with a specific input variable (i.e., the individual wavelength), against the performance obtained at the same conditions with a baseline algorithm. The baseline algorithm used for this comparison was the ZeroR learner, which calculates the average value of the measured variables and uses it as a prediction. This algorithm is considered the baseline for the Weka library of machine learning classifiers. A Metric score, related to this difference in performance between

algorithms is obtained from this approach. In this regard, this score can be positive or negative, and even return a number above 1 (since the increase may exceed 100%).

We used the Metric score to indicate the most contributive spectral wavelengths for the prediction. The intention behind it is to provide information related to the importance of these variables in separating undamaged plants from different insect-type damaged plants, evaluated in our dataset. To help ascertain the most contributive spectral regions instead of only the individual contribution of our data, we implemented a clustering algorithm, based on an unsupervised artificial neural network, known as the Self-Organizing Map (SOM). The SOM applies a competitive learning approach using a neighborhood function. This helps to preserve the topological properties of the input variables, and it is useful for evaluating as it creates a low-dimensional visualization of high-dimensional data. The SOM was executed with 1000 and 2000 epochs in, respectively, the ordering and convergence phases. A height of lattice equal to 2, a learning rate of 1.0, and the normalization of the attributes were also used in this task. With that, we plotted the feature maps of the Metric score and identified the highest contributive spectral regions used by the machine learning algorithm to model it.

### 3. Results

The initial dataset was composed of all measure variables within the days of analysis and separated into two classes: Undamaged plants (UDP) and herbivory-damaged plants (with *S. frugiperda* larvae and *D. melacanthus*). The prediction using the described dataset was executed with 8 machine learning algorithms, and the results indicated a significant overall better performance with the Random Forest (RF) learner (Fig. 2 and Table 2). Here, we compared both the Precision, Recall, and F-Measures among the algorithms, and adopted Scott-Knott test to indicate the differences between the mean values of each prediction.

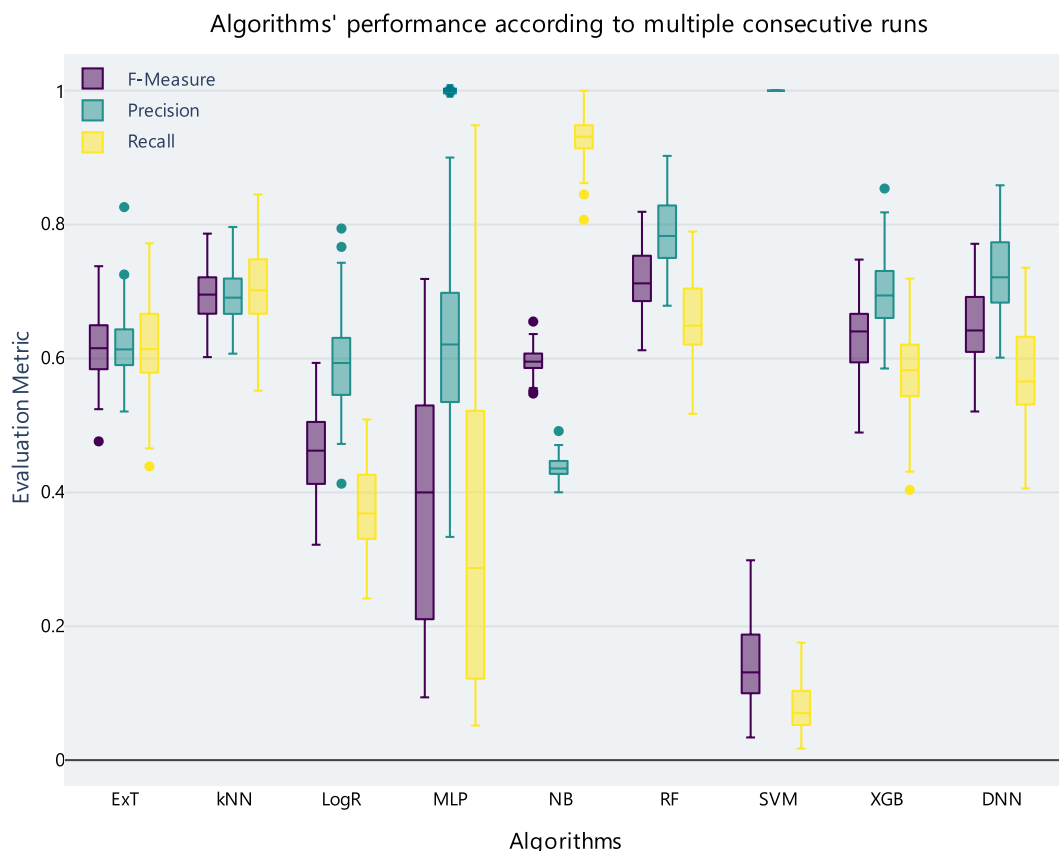


Fig. 2. Models’ performance comparison considering undamaged and insect-damaged maize plants with 8 consecutive days of insect-damage.

**Table 2**

Algorithms comparison considering undamaged and insect-damaged maize plants at all days of analysis. Metric values followed by different letters indicate a significant difference between each algorithm at the training dataset by the Scott-Knott test at 5% probability.

Algorithm	Precision	Recall	F-Measure	ROC Area
ExT	69.8% e	69.8% c	69.8% d	68.6% e
kNN	74.8% c	74.6% a	74.7% b	74.1% c
LogR	63.7% f	64.7% d	62.8% e	71.5% d
MLP	61.7% g	61.9% f	61.8% f	67.0% f
NB	56.8% h	47.3% g	43.4% h	53.3% g
RF	78.5% a	78.7% a	78.3% a	85.4% a
SVM	77.1% b	63.0% e	51.5% g	53.9% g
XGB	72.4% d	72.8% b	72.2% c	79.2% b
DNN	44.2% i	39.2% h	42.1% i	48.5% h

Since F-Measure is a harmonic mean between Precision and Recall (Han and Kamber, 2006), we considered it the most important parameter to compare the models. The ROC area for the RF was the highest of all models, indicating that the algorithm returned high true-positives and low false-positives values with more consistency than the others.

We used the RF algorithm, with the same preset configurations from the previous analysis, to evaluate its prediction capability in a day-to-day approach. In this regard, the RF learner was capable of achieving higher accuracy (F-Measure) than when considering all of the datasets, and this is a piece of evidence that the spectral response of maize plants under insect attacks changed significantly over the days. Still, the classification achieved satisfactory performance since day 1, which is an indication of how robust hyperspectral data and machine learning analysis are. To ensure this comparison and highlight some of these aspects, we evaluated both the multiple validation sets returned by our consecutive runs during the training phase, as well as the F-measure returned at the testing phase of the algorithm (Fig. 3).

Since RF returned the overall best predictions on the 5th day of analysis, we chose this configuration set to evaluate the capability of the combination between spectral behavior and learning approach to separate different types of insect damage. We evaluated the spectral average of the individually measured wavelengths, and for the entire

optical region (400 nm to 2500 nm), the near-infrared refers to the most contributive spectral region to segregate undamaged maize plants from damaged ones due to insects' attacks like *S. frugiperda* larvae or *D. melacanthus* (Fig. 4).

In a "one-against-all" type of approach, the RF algorithm was able to separate with high accuracies the three treatments (undamaged plants, Sf-HDP and Dm-HDP). The undamaged plants returned better metrics overall, followed by the Sf-GDP and, later, Dm-HDP (Table 3), and this quantitative finding is corroborated with the visual analysis of wavelengths behavior for each treatment (Fig. 4). This was important to indicate that, even considering similarities between the spectral curves, the model was able to overcome most of it and indicate the correct group.

To determine the individual performance of the RF learner when confronting the different classes in a pairwise manner, we used different subsets with a two-class approach, as indicated in Table 1. This approach demonstrated that it is easier for the algorithm to separate undamaged maize plants from Dm-HDP, and this can be explained by analyzing the spectral difference presented by these two classes (UDP and Dm-HDP) mainly inside the near-infrared region (750 nm to 1200 nm) (Fig. 4). RF was also capable of differentiating between maize plants from caterpillar (*Spodoptera frugiperda*) to bug (*Dichelops melacanthus*) attack, much like when grouping the three classes (Table 3). The testing metrics also indicated interesting information for the different scenarios considered (Table 4). Both qualitative and quantitative analysis shows that as the classes (for example Dm-HDP and Sf-HDP) present lesser spectral differences (Fig. 4) more difficulties the algorithm found to segregate them (Table 3).

Since the RF learner performs multiple combinations of the wavelengths used, it is difficult to evaluate its predictions pattern. In this sense, the ranking approach combined with the Self-Organizing Map (SOM) method was chosen to ascertain its relationship with the input variables. Here, this framework was implemented with the subsets separated into the pairwise comparison manner (Fig. 5). The highlighted areas in yellowish-circles indicate the most contributive regions, with less interference from other clusters.

The addition of the SOM method helped to indicate which regions

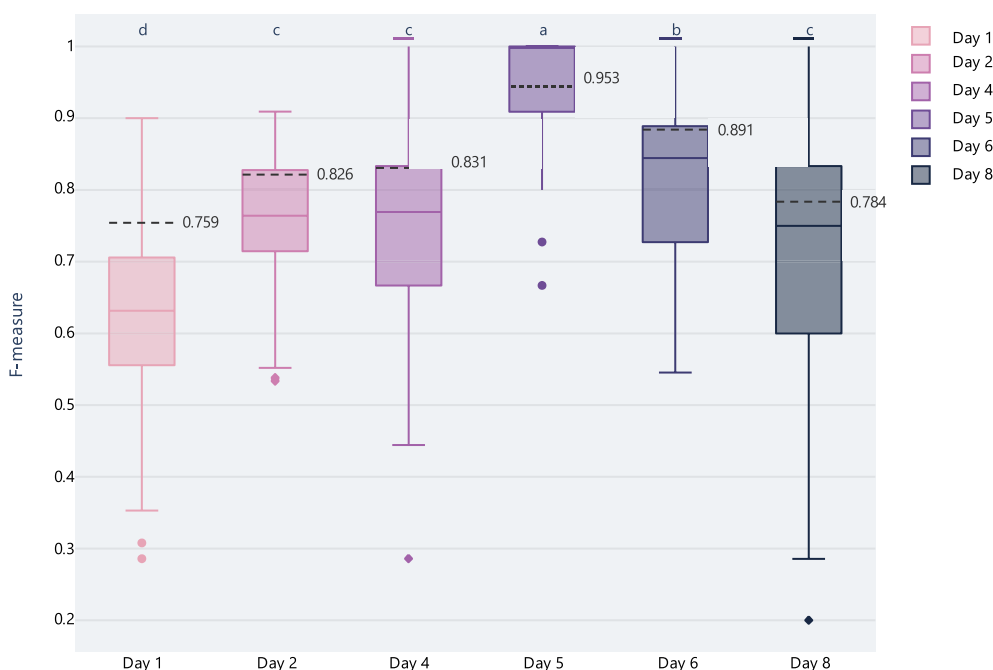


**Fig. 3.** Random Forest (RF) performance metric comparison between days of analysis considering undamaged and insect-damaged maize plants. Letters positioned above the metric value indicate the differences between each day's prediction. The value highlighted inside the box-plot regions corresponds with the F-measure returned at the testing phase.

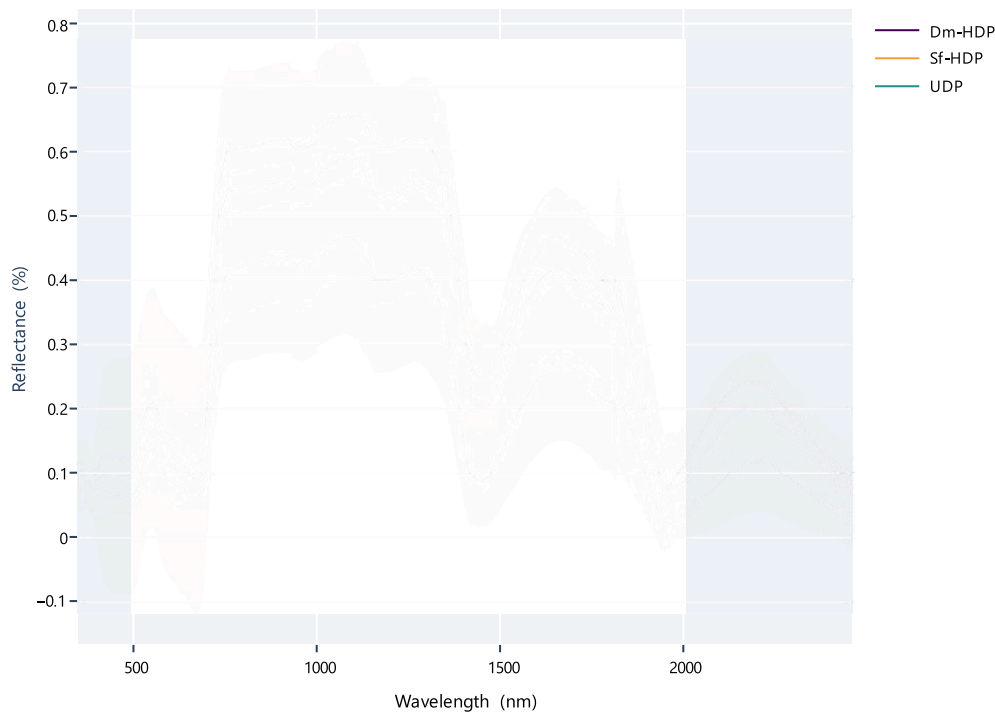


Fig. 4. Spectral wavelengths for the three classes (undamaged plants - UDP, Sf-HDP, and Dm-HDP) measured on day 5 of the analysis.

Table 3

Evaluation metrics returned by the Random Forest algorithm for separating all the classes on day 5.

Group	Precision	Recall	F-Measure	ROC Area
UDP	96.7%	96.7%	96.7%	98.9%
Sf-HDP	95.7%	88.0%	91.7%	97.0%
Dm-HDP	84.1%	92.5%	88.1%	97.0%

Table 4

Testing metrics (averaged values) of each classification for separating UDP (undamaged maize plants), Sf-HDP and Dm-HDP.

Treatments	TP Rate	FP Rate	Precision	Recall	F-Measure
UDP vs Sf-HDP	96.4%	04.0%	96.4%	96.4%	96.4%
UDP vs Dm-HDP	96.0%	04.3%	96.0%	96.0%	96.0%
Sf-HDP vs Dm-HDP	84.4%	14.9%	84.9%	84.4%	84.5%

should be isolated by considering the cluster constructed with the highest Metric values (cluster 3 in Fig. 5). These regions can be defined by their higher contribution to the RF models prediction, and also with lesser interference from the wavelengths grouped into inferior clusters (clusters 2, 1, and 0). To summarize the metric values related to the defined regions with the help of the SOM method, we calculate a descriptive analysis of the spectral regions (Table 5).

Here, the highest average metric values were obtained, interestingly enough, for the comparison between control and caterpillar groups instead of control and bug groups comparison. The graphical (Fig. 5) and descriptive (Table 5) analysis shows that the visible region (400 nm to 650 nm) can not segregate damaged maize plants by Sf-HDP and Dm-HDP. It occurs since damaged plants have their biophysical and biological parameters altered like chlorophyll production (Jensen, 2014; Asner, 1998) compared to undamaged ones, which is reflected in the spectral response of plants for blue and red regions mainly.

#### 4. Discussion

When individually evaluating the performance of each algorithm, the kNN and XGB returned high accuracies, and the Recall mean value obtained with the kNN was higher than RFs'. However, since the Precision values of RF were higher, the harmonic measure (F) was higher for this classifier. SVM and NB returned the worst results, and although SVM presented a Precision equal to 1 in all of the validations' set (Fig. 2), which is due to an overestimate of one of the classes (damage group) above the other (control group), this scenario resulted in the lowest Recall possible. In the testing phase (Table 2) the SVM method presented a more leveled classification. Regardless, it returned one of the worst possible outcomes. Additionally, in the testing phase, the DNN model was significantly worse than the remaining models, which indicated an overfitting during the training and validation phase (Fig. 2). Regardless, there is potential for deep learning models in spectra data, and future investigations should require different takes on this issue. In our case, while the DNN did not resulted in a satisfactory result, other algorithms like RF were better to our data characteristics.

The comparison between shallow and deeper approaches is an important task when investigating different algorithms, and although deep models are recognized as more powerful and robust methods than shallow learners (Osco et al., 2021), there are characteristics in the dataset that dictates how well these models can perform. In this case, our hypothesis for the DNN performing worse than the machine learning methods was not only related to the sample size used (n = 1,429), but how redundant some of the spectral wavelengths may be within the dataset. Besides, another possible explanation relates to the high dimensionality of the data (1,934 attributes, from different waves between 350 and 2,500 nm), also described as the curse of dimensionality (known as Hughes phenomenon) (Miyoshi et al., 2020). The RF algorithm is considered one of the most powerful algorithms in use, and its capability of learning from multiple input variables is something that is benefited from a highly-dimensional dataset such as this one (Breiman, 2001).

In other study related to spectral readings and agronomic-related predictions with machine learning methods, RF was able to infer both

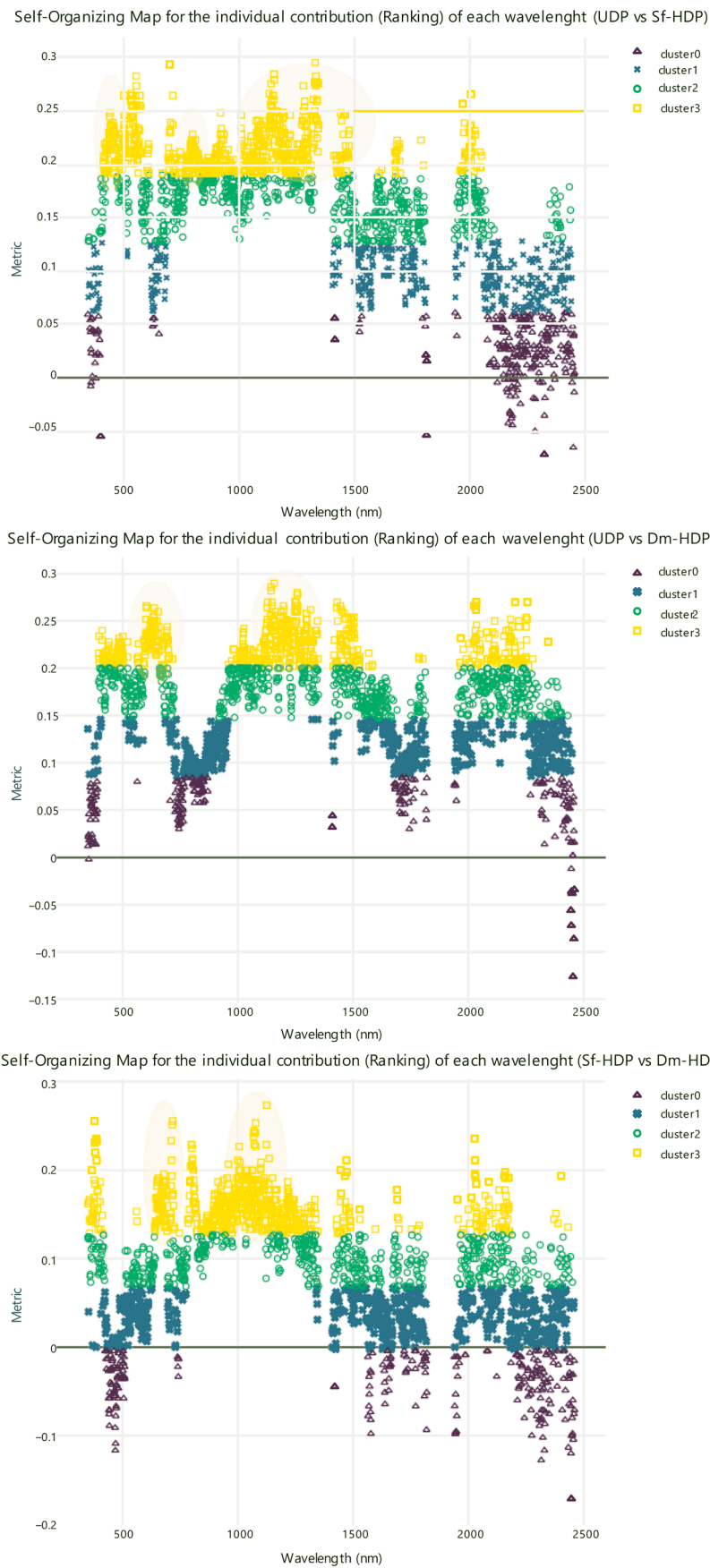


Fig. 5. Ranking metric and SOM clustering method indicating the importance of wavelengths for the three maize plant experiments.



**Table 5**

Returned metric values for the spectral regions defined with the help of Ranking + SOM method using the spectral measures from the three treatments - Undamaged plants (UDP), Plants with an injury of two *S. frugiperda* larvae (SF-HDP), and from plants with an injury of two *D. melacanthus*.

Comparison	Spectral Regions	Min. Metric	Average Metric	Max. Metric
UDP vs Sf-HDP	420–480, 500–580, and 780–1350 nm	0.191	0.215 +- 0.020	0.294
UDP vs Dm-HDP	600–660 and 1100–1350 nm	0.148	0.177 +- 0.015	0.2
Sf-HDP vs Dm-HDP	640–700 and 900–1250 nm	0.098	0.098 +- 0.017	0.069

macro and micronutrients in hyperspectral readings with satisfactory performances (Osco et al., 2020b). The algorithm was also used in the hyperspectral imagery-domain to predict weed presence in maize-crops (Gao et al., 2018) and vegetable crop biomass with Unmanned Aerial Vehicle (UAV) type of data (Astor et al., 2020). Regarding insect-damage detection in crops, the accuracy achieved here was approximate from the values obtained by the other methods (Wang et al., 2011; Liu et al., 2018; Tageldin et al., 2020). Although from day 4 and beyond the RF model already returned high values, the analysis on day 5 achieved the overall best prediction, with some outliers below 0.80. The testing results indicated, from the 2nd day of the insect-attack, it is possible to achieve high prediction values with RF to separate undamaged from insect-damaged maize plants. This information is interesting since it is an indication of how the reflectance measurements from proximal sensing, alongside the robustness of the RF algorithm, are sensitive to the effects of the insect-attack in maize plants.

The pattern returned by the conducted analyses indicates that it is easier for the algorithm to separate bug (*Dichelops melacanthus*) attacks than caterpillar (*Spodoptera frugiperda*) attacks from undamaged maize plants. And although it is possible to achieve high accuracies in separating the insect-type of attack by comparing the bug group against the *Spodoptera frugiperda* group, it is, as expected, more difficult than when in comparison with undamaged plants. This is probably related to how both spectral curves (Fig. 4) behave for the different types of classes. The *Dichelops melacanthus* and control averaged curves are far apart from each other, while the averaged curve from caterpillar attacked maize plants is in between them, with a high standard deviation.

In some regions (Fig. 4), the averaged spectral curves of bug and caterpillar groups are almost near each other. In general, lepidopteran larvae can induce higher levels of injury in plant tissues when compared to stink bugs, which are sucking insects. Studies have shown that maize plants can have their direct defense response suppressed by *S. frugiperda* larvae (Wouters et al., 2016). *S. frugiperda* can manipulate the plant defense in its favor (Glaser et al., 2011) minimizing the production of toxic compounds. On the other hand, herbivory injury of *D. melacanthus* herbivory in maize plants induces direct plant defense during the first 24 h of herbivory. Similar results were observed by (Glaser et al., 2011) when *S. frugiperda* larvae at the fourth instar feed on maize plants. The higher changes in the chemical profile of direct defense in maize plants injury by herbivory of the stink bug compared to larvae of *S. frugiperda* support the better separation obtained by the algorithm.

As for the individual contribution of the wavelengths, the ranking approach combined with the Self-Organizing Map (SOM) method is, in the presented sense, a newly developed approach that can help with the analysis to indicate the most important wavelengths and spectral regions used for the classification performed by the machine learning algorithm. This highlights the importance of the input data (wavelengths) and how well they respond to the algorithms' modeling. The ranking approach in the machine learning context is normally used as a pre-processing step to reduce the number of input variables to the models by selecting only the most important data. In agricultural related problems, we implemented this type of approach with the RF and other learners (Ramos et al., 2020;

Osco et al., 2020a), and it returned important data to monitor maize-yield, canopy nitrogen content in citrus and leaf nitrogen concentration and plant height in maize plants too. Also in this aspect, when implementing this type of approach for proximal sensing, a different concept with the Relief-F method (Osco et al., 2020a) was considered for mapping both macro and micronutrients in citrus-trees. Yet, by adopting the Metric score calculation after the algorithms' classification, it is possible to measure how well each wavelength relates to the performance of the algorithm.

The identification of isolated spectral regions is an important feature to be incorporated into studies that aim to evaluate different types of behavior in plants. The main idea behind it is to propose more direct and clear spectral bands to be associated with the respective problem. Our model focused on insect-damage in maize plants, however, the proposed framework should be possible to be implemented in related research. It could also be considered into novel studies that aim to develop simpler and direct methods to estimate these variables, such as spectral vegetation indices, or even sensors and equipment that focus on these particular spectral regions.

Although it may be related to the model predictor (being this case, the RF learner), we intend to perform further investigations to compare more traditional methods with the machine learning algorithm to better ascertain the impact related to this reduction in data-dimensionality. Another possibility is that the information presented, obtained with proximal measurements at wavelength scale, can be implemented in other projects that aim to evaluate the impact of the spectral regions on detecting insect-damage in imagery sensors embedded in UAV platforms. These platforms are capable of embedding hyperspectral sensors and achieve high-spatial resolutions, providing spectral information at plant level. Novel research that intends to apply and improve this framework, must consider the challenges in which the differences between proximal sensing and aerial sensing impose. Regardless, when calculating image data at reflectance values, a similar conduct can be investigated to separate undamaged plants from others attacked by such insects.

## 5. Conclusions

The main contribution of this study was to present an approach with machine and deep learning based models to detect and separate insect-damaged plants from undamaged maize plants using only the reflectance measurements obtained with a proximal hyperspectral sensing approach. We indicated which learner was more efficient to evaluate the impact of a day-by-day analysis. Lastly, we proposed a novel framework to identify important spectral regions from visible to short-wave infrared bands (from 350 to 2500 nm) using a combination of ranking and self-organizing map (SOM) approaches. Our results indicated that the RF algorithm is the overall best learner to deal with. After the 5th day of analysis, the accuracy of the RF algorithm improved substantially. It separated the control, caterpillar (*Spodoptera frugiperda*), and bug (*Dichelops melacanthus*) groups with an F1-measure equal to 96.7%, 91.7%, and 88.1%, respectively. Our approach also reveals that the most contributive spectral regions are situated in the near-infrared domain and, on a small scale, in red, green, and blue, in this respective order. We conclude that the approach with machine learning methods is adequate to monitor insect-damage in maize plants, differentiating the types of insect attack early on. We demonstrate that indicating the most contributive wavelengths is suitable to highlight spectral regions of interest. We hope that future research adopts the proposal presented herein for other types of cultivars and cultures.

## Funding

This research was partially funded by National Council for Scientific and Technological Development (CNPq), project number: 433783/2018-4, 303559/2019-5, 304052/2019-1, and 310517/2020-6, also

received financial support from the Brazilian Corporation of Agricultural Research (EMBRAPA), project number: 11.14.09.001.04.00, and moreover was also partially supported by the Emerging Interdisciplinary Project of Central University of Finance and Economics from China.

### Declaration of Competing Interest

The authors declare that they have no known competing financial interests or personal relationships that could have appeared to influence the work reported in this paper.

### Acknowledgments

The authors acknowledge the support of the Coordenação de Aperfeiçoamento de Pessoal de Nível Superior (CAPES) (Finance Code 001).

### References

- Abdulridha, J., Batuman, O., Ampatzidis, Y., 2019. UAV-based remote sensing technique to detect citrus canker disease utilizing hyperspectral imaging and machine learning. *Remote Sensing* 11, 1373. <https://doi.org/10.3390/rs11111373>.
- Asner, G.P., 1998. Biophysical and biochemical sources of variability in canopy reflectance. *Remote Sens. Environ.* 64, 234–253. [https://doi.org/10.1016/S0034-4257\(98\)00014-5](https://doi.org/10.1016/S0034-4257(98)00014-5). URL: <https://www.sciencedirect.com/science/article/pii/S0034425798000145>.
- Assefa, F., Ayalew, D., 2019. Status and control measures of fall armyworm (spodoptera frugiperda) infestations in maize fields in ethiopia: A review. *Cogent Food Agric.* 5, 1641902. <https://doi.org/10.1080/23311932.2019.1641902> arXiv:<https://doi.org/10.1080/23311932.2019.1641902>.
- Astor, T., Dayananda, S., Nautiyal, S., Wachendorf, M., 2020. Vegetable crop biomass estimation using hyperspectral and RGB 3d UAV data. *Agronomy* 10, 1600. <https://doi.org/10.3390/agronomy10101600>.
- Berger, K., Verrelst, J., Féret, J.B., Hank, T., Woche, M., Mauser, W., Camps-Valls, G., 2020. Retrieval of aboveground crop nitrogen content with a hybrid machine learning method. *Int. J. Appl. Earth Obs. Geoinf.* 92, 102174. <https://doi.org/10.1016/j.jag.2020.102174>. URL: <https://www.sciencedirect.com/science/article/pii/S0303243420303500>.
- Breiman, L., 2001. Random forests. *Machine Learn.* 45, 5–32. <https://doi.org/10.1023/a:1010933404324>.
- CONAB, 2020. Monitoring of the brazilian harvest 2019/2020.
- El-Ghany, N.M.A., El-Aziz, S.E.A., Marei, S.S., 2020. A review: application of remote sensing as a promising strategy for insect pests and diseases management. *Environ. Sci. Pollut. Res.* 27, 33503–33515. <https://doi.org/10.1007/s11356-020-09517-2>.
- Gao, J., Nuyttens, D., Lootens, P., He, Y., Pieters, J.G., 2018. Recognising weeds in a maize crop using a random forest machine-learning algorithm and near-infrared snapshot mosaic hyperspectral imagery. *Biosyst. Eng.* 170, 39–50. <https://doi.org/10.1016/j.biosystemseng.2018.03.006>.
- Glauser, G., Marti, G., Villard, N., Doyen, G.A., Wolfender, J.L., Turlings, T.C., Erb, M., 2011. Induction and detoxification of maize 1, 4-benzoxazin-3-ones by insect herbivores. *Plant J.* 68, 901–911. <https://doi.org/10.1111/j.1365-3113x.2011.04740.x>.
- Han, J., Kamber, M., 2006. *Data Mining Concept and Tehniques*. Morgan Kaufman, San Francisco.
- Jensen, J.R., 2014. *Remote Sensing of the Environment: An Earth Resource Perspective*, second ed., vol. 1. Prentice Hall.
- Kandpal, L.M., Lee, S., Kim, M.S., Bae, H., Cho, B.K., 2015. Short wave infrared (SWIR) hyperspectral imaging technique for examination of aflatoxin b1 (AFB1) on corn kernels. *Food Control* 51, 171–176. <https://doi.org/10.1016/j.foodcont.2014.11.020>.
- Kohonen, T., 1982. Self-organized formation of topologically correct feature maps. *Biol. Cybern.* 43, 59–69. <https://doi.org/10.1007/bf00337288>.
- Kohonen, T., 2001. *Self-Organizing Maps*. Springer, Berlin Heidelberg. <https://doi.org/10.1007/978-3-642-56927-2>.
- Li, Y., Wright, A., Liu, H., Wang, J., Wang, G., Wu, Y., Dai, L., 2019. Land use pattern, irrigation, and fertilization effects of rice-wheat rotation on water quality of ponds by using self-organizing map in agricultural watersheds. *Agric. Ecosyst. Environ.* 272, 155–164. <https://doi.org/10.1016/j.agee.2018.11.021>.
- Liu, Z.Y., Qi, J.G., Wang, N.N., Zhu, Z.R., Luo, J., Liu, L.J., Tang, J., Cheng, J.A., 2018. Hyperspectral discrimination of foliar biotic damages in rice using principal component analysis and probabilistic neural network. *Precision Agric.* 19, 973–991. <https://doi.org/10.1007/s11119-018-9567-4>.
- Mahlein, A.K., 2016. Plant disease detection by imaging sensors – parallels and specific demands for precision agriculture and plant phenotyping. *Plant Dis.* 100, 241–251. <https://doi.org/10.1094/pdis-03-15-0340-fe>.
- Miyoshi, G.T., dos Santos Arruda, M., Osco, L.P., Junior, J.M., Gonçalves, D.N., Imai, N. N., Tommaselli, A.M.G., Honkavaara, E., Gonçalves, W.N., 2020. A novel deep learning method to identify single tree species in UAV-based hyperspectral images. *Remote Sensing* 12, 1294. <https://doi.org/10.3390/rs12081294>.
- Nyabako, T., Mvumi, B.M., Stathers, T., Mlambo, S., Mubayiwa, M., 2020. Predicting prosthephanus truncatus (horn) (coleoptera: Bostrichidae) populations and associated grain damage in smallholder farmers' maize stores: A machine learning approach. *J. Stored Prod. Res.* 87, 101592. <https://doi.org/10.1016/j.jspr.2020.101592>.
- Oliveira, C., Auad, A., Mendes, S., Frizzas, M., 2014. Crop losses and the economic impact of insect pests on brazilian agriculture. *Crop Protection* 56, 50–54. <https://doi.org/10.1016/j.cropro.2013.10.022>.
- Osco, L.P., Junior, J.M., Ramos, A.P.M., Furuya, D.E.G., Santana, D.C., Teodoro, L.P.R., Gonçalves, W.N., Baio, F.H.R., Pistori, H., Junior, C.A.d.S., Teodoro, P.E., 2020a. Leaf nitrogen concentration and plant height prediction for maize using uav-based multispectral imagery and machine learning techniques. *Remote Sensing* 12. <https://doi.org/10.3390/rs12193237>. URL: <https://www.mdpi.com/2072-4292/12/19/3237>.
- Osco, L.P., Marcato Junior, J., Marques Ramos, A.P., de Castro Jorge, L.A., Fathollahi, S. N., de Andrade Silva, J., Matsubara, E.T., Pistori, H., Gonçalves, W.N., Li, J., 2021. A review on deep learning in uav remote sensing. *Int. J. Appl. Earth Obs. Geoinf.* 102, 102456. <https://doi.org/10.1016/j.jag.2021.102456>. URL: <https://www.sciencedirect.com/science/article/pii/S0303243421100163X>.
- Osco, L.P., Ramos, A.P.M., Moriya, É.A.S., de Souza, M., Junior, J.M., Matsubara, E.T., Imai, N.N., Creste, J.E., 2019. Improvement of leaf nitrogen content inference in valencia-orange trees applying spectral analysis algorithms in UAV mounted-sensor images. *Int. J. Appl. Earth Obs. Geoinf.* 83, 101907. <https://doi.org/10.1016/j.jag.2019.101907>.
- Osco, L.P., Ramos, A.P.M., Pinheiro, M.M.F., Moriya, É.A.S., Imai, N.N., Estrabis, N., Ianczyk, F., de Araújo, F.F., Liesenberg, V., de Castro Jorge, L.A., Li, J., Ma, L., Gonçalves, W.N., Junior, J.M., Creste, J.E., 2020b. A machine learning framework to predict nutrient content in valencia-orange leaf hyperspectral measurements. *Remote Sensing* 12, 906. <https://doi.org/10.3390/rs12060906>.
- Ramos, A.P.M., Osco, L.P., Furuya, D.E.G., Gonçalves, W.N., Santana, D.C., Teodoro, L.P.R., da Silva Junior, C.A., Capristo-Silva, G.F., Li, J., Baio, F.H.R., Junior, J.M., Teodoro, P.E., Pistori, H., 2020. A random forest ranking approach to predict yield in maize with uav-based vegetation spectral indices. *Comput. Electron. Agric.* 178, 105791. <https://doi.org/10.1016/j.compag.2020.105791>.
- Rivas-Tabares, D., de Miguel, A., Willaarts, B., Tarquis, A.M., 2020. Self-organizing map of soil properties in the context of hydrological modeling. *Appl. Math. Model.* 88, 175–189. <https://doi.org/10.1016/j.apm.2020.06.044>.
- Schmidt, L., Schurr, U., Röse, U.S.R., 2009. Local and systemic effects of two herbivores with different feeding mechanisms on primary metabolism of cotton leaves. *Plant, Cell Environ.* 32, 893–903. <https://doi.org/10.1111/j.1365-3040.2009.01969.x>.
- Silver, A., 2019. Caterpillar's devastating march across china spurs hunt for native predator. *Nature* 570, 286–287. <https://doi.org/10.1038/d41586-019-01867-3>.
- Singh, C., Jayas, D., Paliwal, J., White, N., 2009. Detection of insect-damaged wheat kernels using near-infrared hyperspectral imaging. *J. Stored Prod. Res.* 45, 151–158. <https://doi.org/10.1016/j.jspr.2008.12.002>.
- Singh, V., Sharma, N., Singh, S., 2020. A review of imaging techniques for plant disease detection. *Artif. Intell. Agric.* 4, 229–242. <https://doi.org/10.1016/j.aiia.2020.10.002>.
- Tageldin, A., Adly, D., Mostafa, H., Mohammed, H.S., 2020. Applying machine learning technology in the prediction of crop infestation with cotton leafworm in greenhouse. *bioRxiv* <https://doi.org/10.1101/2020.09.17.301168>.
- Wang, J., Nakano, K., Ohashi, S., Kubota, Y., Takizawa, K., Sasaki, Y., 2011. Detection of external insect infestations in jujube fruit using hyperspectral reflectance imaging. *Biosyst. Eng.* 108, 345–351. <https://doi.org/10.1016/j.biosystemseng.2011.01.006>.
- Wouters, F.C., Blanchette, B., Gershenzon, J., Vassão, D.G., 2016. Plant defense and herbivore counter-defense: benzoxazinoids and insect herbivores. *Phytochem. Rev.* 15, 1127–1151. <https://doi.org/10.1007/s11101-016-9481-1>.
- Zhang, D., Ding, Y., Chen, P., Zhang, X., Pan, Z., Liang, D., 2020. Automatic extraction of wheat lodging area based on transfer learning method and deeplabv3/mathplus network. *Comput. Electron. Agric.* 179, 105845. <https://doi.org/10.1016/j.compag.2020.105845>.
- Zhang, J., Huang, Y., Pu, R., Gonzalez-Moreno, P., Yuan, L., Wu, K., Huang, W., 2019. Monitoring plant diseases and pests through remote sensing technology: A review. *Comput. Electron. Agric.* 165, 104943. <https://doi.org/10.1016/j.compag.2019.104943>.